GST-PRX5$_{68-90}$, GST-PRX6$_{66-93}$: peptides contained β4 sheet and α3 helix regions). IL-23p19 mRNA levels were detected by means of quantitative RT-PCR in BMDC 1 hour after stimulation with 1 μM recombinant proteins. (**c,d**) Infarct volume on day 4 (bar: 1 mm) (**c**) and neurological scores (**d**) on days 1 and 3 of mice treated with control IgG or anti-Prx5, Prx6 antibody mixture or anti-Prx5 $_{68-90}$, Prx6 $_{66-93}$ (common α3 helix and β4 sheet region) antibody mixture immediately after the induction of brain ischemia (300 μg/mouse). $^{*}p < 0.05$, $^{**}p < 0.01$, $^{***}p < 0.001$ vs. GST-PRX5 $_{1-162}$ (**a**) and control IgG-treated mice (**c,d**) (one-way ANOVA with Dunnett's correction; the error bars represent s.e.).

Methods

Mice. TLR2-KO, TLR4-KO, TLR2/4-DKO, MyD88-KO, and TRIF-KO mice were kindly provided by Dr. K Miyake and Dr. S Akira. Prx1-KO mice were kindly provided by Dr. T Ishii. All mice were from a C57BL/6 background. All experiments were approved by the Institutional Animal Research Committee of Keio University (approval number: 08004).

Murine focal brain ischemia model. Male mice, aged 9 to 12 weeks and weighing 20–30 g, were used for focal brain ischemia experiments. There was no significant difference in weight and age between WT mice and any of the KO groups. We used a transient middle cerebral artery occlusion (MCAO) model induced by means of an intraluminal suture. The method of inducing this transient suture MCAO model has been described previously[11,47]. A greater-than-60% reduction in cerebral blood flow was confirmed by laser Doppler flowmetry, and head temperature was kept at 36°C using a heat lamp.

Sixty minutes after MCAO, the brain was reperfused by the withdrawal of the intraluminal suture.

At the indicated time points after MCAO, neurological function was evaluated using a previously described 4-point-scale neurological score method[11]. For measurement of the infarct volume, the mice were fixed by transcardial perfusion with cold PBS followed by 4% paraformaldehyde/PBS. We embedded 1-mm-thick serial coronal slices from the brains in paraffin sections and immunostained them with MAP2-specific antibody. To determine the border of infarcted and non-infarcted regions at early time points after stroke onset, we examined the nuclear morphological change of neuronal cells stained with DAPI and also performed TUNEL-staining.

Preparation and LC/MS analysis of brain lysate. The mice were perfused with PBS transcardially. The forebrain was removed, homogenized with RPMI-1640, and centrifuged at 15,000 rpm for 5 min. The supernatant was made up to 1 ml with RPMI-1640 and used as the brain lysate. For the pronase and DNaseI digestion assay, the brain lysate was incubated with pronase (1-10 U ml^{-1}, Roche) or DNase I (50 μg ml^{-1}, Roche) at 37°C for 1 hour.

For the sucrose density gradient centrifugation and LC/MS analysis, the brain lysate was ultracentrifuged at 47,000 rpm for 1 hour. The supernatant was applied to DEAE Sepharose Fast Flow (GE Healthcare), and the flow through was condensed by ultrafiltration with an Amicon Ultra-4 Centrifugal Filter Unit with Ultracel-10 membrane (Millipore). Four hundred microliters of condensed solution was layered on a 1-ml 10–40% (w/w) linear sucrose gradient in PBS, and centrifuged at 40,000 rpm for 12 hours. Sucrose was depleted by ultrafiltration from each of the sucrose gradient fractions. We added each of the sucrose gradient fractions to a culture of BMDC to examine its capacity to induce

inflammatory cytokines and analyzed sucrose gradient fractions No. 1–4 by means of LC/MS. LC/MS analysis was performed after trypsin treatment using a Qstar-XL mass spectrometer (Applied Biosystems).

For the antibody-depletion assay, HMGB1 or Prx proteins were depleted by immunoprecipitation with antibody cross-linked Protein G beads using dimethyl pimelimidate (DMP). Depletion of HMGB1 or Prx proteins from the brain lysate was confirmed by Western blot analysis.

Generation of recombinant protein. cDNA clones encoding candidate proteins identified by LC/MS analysis were cloned from a mouse brain cDNA library. All mutations were made with complementary mutagenic oligonucleotides. Final cDNA constructs were inserted into the pGEX6P-3 plasmid (GE Healthcare) and expressed as GST fusion proteins in BL21 competent cells (Stratagene). Following fusion protein purification using Glutathione-Sepharose 4B (GE Healthcare), 100 μl of protein-bound glutathione beads were extensively washed with 10 ml of cold PBS five times. Washed protein-bound glutathione beads were either eluted with 20 mM reduced glutathione (pH 8.0) to elute GST-fusion proteins or incubated with PreScission Protease (GE Healthcare) overnight at 4°C to remove the GST tag. Finally, these recombinant proteins were incubated with Affi-Prep Polymyxin Support (Bio-Rad) for 12 hours at 4°C to remove endotoxins and endotoxin-bound proteins. We confirmed through SDS-PAGE and CBB staining that the same amounts of purified recombinant proteins were applied to BMDC stimulation experiments. Recombinant GST protein was always used as a negative control for cytokine induction in BMDC.

To generate alkylated Prx proteins, recombinant Prx protein with 1 mM dithiothreitol (DTT) was incubated with 55 mM iodoacetamide (Wako Pure

Chemical Industries Ltd.) in a dark chamber at room temperature for 1 hour. Sufficient alkylation of -SH residues in Prx protein was confirmed using dithionitrobenzoic acid (Dojindo Laboratories).

Generation of rabbit polyclonal antibody. Rabbits were immunized with recombinant Prx proteins by Japan Lamb. To affinity-purify antibodies, recombinant Prx proteins were crosslinked to NHS-Sepharose beads. The Protein A-purified antibodies from immunized rabbit serum were applied to Prx protein-bound NHS-Sepharose beads. These affinity-purified antibodies were used for all experiments in this study.

Anti-HMGB1 antibody. Anti-HMGB1 antibody (rat, monoclonal) was kindly provided by Dr. H Takahashi, Dr. S Mori, and Dr. M Nishibori. As previously reported, 200 μg of anti-HMGB1 antibody was administered immediately or 6 hours after the induction of brain ischemia[20,45].

Statistical analysis. Data are expressed as means ± the standard error (s.e.). We performed a one-way analysis of variance (ANOVA) followed by post hoc multiple comparison tests (Dunnett's correction) to analyze differences among three or more groups of mice. Between two groups of mice, an unpaired Student's *t*-test was performed to determine statistical significance. $p < 0.05$ was considered a significant difference.

References

1 Moskowitz MA, Lo EH, Iadecola C. The science of stroke: mechanisms in search of treatments. *Neuron.* **67**, 181-198 (2010)

2 Lo EH. Degeneration and repair in central nervous system disease. *Nat Med.*

16, 1205-1209 (2010)

3 Ooboshi *et al.* Postischemic gene transfer of interleukin-10 protects against both focal and global brain ischemia. *Circulation.* **111**, 913-919 (2006)

4 Macrez R, *et al.* Stroke and the immune system: from pathophysiology to new therapeutic strategies. *Lancet Neurol.* **10**, 471-480 (2011)

5 Iadecola C, Anrather J. The immunology of stroke: from mechanisms to translation. *Nat Med.* **17**, 796-808 (2011)

6 Eltzschig HK, Eckle T. Ischemia and reperfusion—from mechanism to translation. *Nat Med.* **17**, 1391-1401 (2011)

7 Hurn PD, *et al.* T- and B-cell-deficient mice with experimental stroke have reduced lesion size and inflammation. *J Cereb Blood Flow Metab.* **27**, 1798-1805 (2007)

8 Liesz A, *et al.* Inhibition of lymphocyte trafficking shields the brain against deleterious neuroinflammation after stroke. *Brain.* **134**, 704-720 (2011)

9 Yilmaz G, Arumugam TV, Stokes KY, Granger DN. Role of T lymphocytes and interferon-gamma in ischemic stroke. *Circulation.* **113**, 2105-2112 (2006)

10 Ren X, *et al.* Regulatory B cells limit CNS inflammation and neurologic deficits in murine experimental stroke. *J Neurosci.* **31**, 8556-8563 (2011)

11 Shichita T, *et al.* Pivotal role of cerebral interleukin-17-producing gammadeltaT cells in the delayed phase of ischemic brain injury. *Nat Med.* **15**, 946-950 (2009)

12 Konoeda F, *et al.* Therapeutic effect of IL-12/23 and their signaling pathway blockade on brain ischemia model. *Biochem Biophys Res Commun.* **402**, 500-506 (2010)

13 Tang SC, *et al.* Pivotal role for neuronal Toll-like receptors in ischemic brain injury and functional deficits. *Proc Natl Acad Sci U S A.* **104**, 13798-13803 (2007)

14 Brea D, *et al.* Toll-like receptors 2 and 4 in ischemic stroke: outcome and therapeutic values. *J Cereb Blood Flow Metab.* **31**, 1424-1431 (2011)

15 Yanai H, *et al.* HMGB proteins function as universal sentinels for nucleic-acid-mediated innate immune responses. *Nature.* **462**, 99-103 (2009)

16 Marsh BJ, Williams-Karnesky RL, Stenzel-Poore MP. Toll-like receptor signaling in endogenous neuroprotection and stroke. *Neuroscience.* **158**, 1007-1020 (2009)

17 Stewart CR, *et al.* CD36 ligands promote sterile inflammation through assembly of a Toll-like receptor 4 and 6 heterodimer. *Nat Immunol.* **11**, 155-161 (2010)

18 Zhang Q, *et al.* Circulating mitochondrial DAMPs cause inflammatory responses to injury. *Nature.* **464**, 104-107 (2010)

19 Rivest S. Regulation of innate immune responses in the brain. *Nat Rev Immunol.* **9**, 429-439 (2009)

20 Zhang J, *et al.* Anti-high mobility group box-1 monoclonal antibody protects the blood-brain barrier from ischemia-induced disruption in rats. *Stroke.* **42**, 1420-1428 (2011)

21 Kim JB, *et al.* HMGB1, a novel cytokine-like mediator linking acute neuronal death and delayed neuroinflammation in the postischemic brain. *J Neurosci.* **26**, 6413-6421 (2006)

22 Yang QW, *et al.* HMBG1 mediates ischemia-reperfusion injury by TRIF-adaptor independent Toll-like receptor 4 signaling. *J Cereb Blood Flow Metab.* **31**, 593-605 (2011)

23 Hayakawa K, Qiu J, Lo EH. Biphasic actions of HMGB1 signaling in inflammation and recovery after stroke. *Ann N Y Acad Sci.* **1207**, 50-57 (2010)

24 Riddell JR, Wang XY, Minderman H, Gollnick SO. Peroxiredoxin 1 stimulates secretion of proinflammatory cytokines by binding to TLR4. *J Immunol.* **184**,

1022-1030 (2010)

25 Chesterman ES, *et al.* Investigation of Prx1 protein expression provides evidence for conservation of cardiac-specific posttranscriptional regulation in vertebrates. *Dev Dyn.* **222**, 459-470 (2001)

26 Patenaude A, Murthy MR, Mirault ME. Emerging roles of thioredoxin cycle enzymes in the central nervous system. *Cell Mol Life Sci.* **62**, 1063-1080 (2005)

27 Hu X, *et al.* Peroxiredoxin-2 protects against 6-hydroxydopamine-induced dopaminergic neurodegeneration via attenuation of the apoptosis signal-regulating kinase (ASK1) signaling cascade. *J Neurosci.* **31**, 247-261 (2011)

28 Rashidian J, *et al.* Essential role of cytoplasmic cdk5 and Prx2 in multiple ischemic injury models, in vivo. *J Neurosci.* **29**, 12497-12505 (2009)

29 Wood ZA, Schröder E, Robin Harris J, Poole LB. Structure, mechanism and regulation of peroxiredoxins. *Trends Biochem Sci.* **28**, 32-40 (2003)

30 Seo MS, *et al.* Identification of a new type of mammalian peroxiredoxin that forms an intramolecular disulfide as a reaction intermediate. *J Biol Chem.* **275**, 20346-20354 (2000)

31 Toohey JI. Sulfhydryl dependence in primary explant hematopoietic cells. Inhibition of growth in vitro with vitamin B12 compounds. *Proc Natl Acad Sci U S A.* **72**, 73-77 (1975)

32 Chou JL, *et al.* Proteomic investigation of a neural substrate intimately related to brain death. *Proteomics.* **11**, 239-248 (2011)

33 Dayon L, *et al.* Brain extracellular fluid protein changes in acute stroke patients. *J Proteome Res.* **10**, 1043-1051 (2011)

34 Jin MH, *et al.* Characterization of neural cell types expressing peroxiredoxins in mouse brain. *Neurosci Lett.* **381**, 252-257 (2005)

35 Chen CJ, *et al.* Identification of a key pathway required for the sterile

inflammatory response triggered by dying cells. *Nat Med.* **13**, 851-856 (2007)

36 Hirotsu S, *et al.* Crystal structure of a multifunctional 2-Cys peroxiredoxin heme-binding protein 23kDa/proliferation-associated gene product. *Proc Natl Acad Sci U S A.* **96**, 12333-12338 (1999)

37 Declercq JP, *et al.* Crystal structure of human peroxiredoxin 5, a novel type of mammalian peroxiredoxin at 1.5 A resolution. *J Mol Biol.* **311**, 751-759 (2001)

38 Choi HJ, *et al.* Crystal structure of a novel human peroxidase enzyme at 2.0 A resolution. *Nat Struct Biol.* **5**, 400-406 (1998)

39 Chen GY, Nuñez G. Sterile inflammation: sensing and reacting to damage. *Nat Rev Immunol.* **10**, 826-837 (2010)

40 Yu M, *et al.* HMGB1 signals through toll-like receptor (TLR) 4 and TLR2. *Shock.* **26**, 174-179 (2006)

41 Triantafilou M, *et al.* Membrane sorting of toll-like receptor (TLR)-2/6 and TLR2/1 heterodimers at the cell surface determines heterotypic associations with CD36 and intracellular targeting. *J Biol Chem.* **281**, 31002-31011 (2006)

42 Yi H, *et al.* Pattern recognition scavenger receptor SRA/CD204 down-regulates Toll-like receptor 4 signaling-dependent CD8 T-cell activation. *Blood.* **113**, 5819-5828 (2009)

43 Akashi-Takamura S, Miyake K. TLR accessory molecules. *Curr Opin Immunol.* **20**, 420-425 (2008)

44 Eismann T, *et al.* Peroxiredoxin-6 protects against mitochondrial dysfunction and liver injury during ischemia-reperfusion in mice. *Am J Physiol Gastrointest Liver Physiol.* **296**, G266-274 (2009)

45 Liu K, *et al.* Anti-high mobility group box 1 monoclonal antibody ameliorates brain infarction induced by transient ischemia in rats. *FASEB J.* **21**, 3904-3916 (2007)

46 Qiu J, *et al.* Early release of HMGB-1 from neurons after the onset of brain

ischemia. *J Cereb Blood Flow Metab.* **28**, 927-938 (2008)

47 Sugimori H *et al.* Krypton laser-induced photothrombotic distal middle cerebral artery occlusion without craniectomy in mice. *Brain Res Protoc.* **13**, 189-196 (2004)

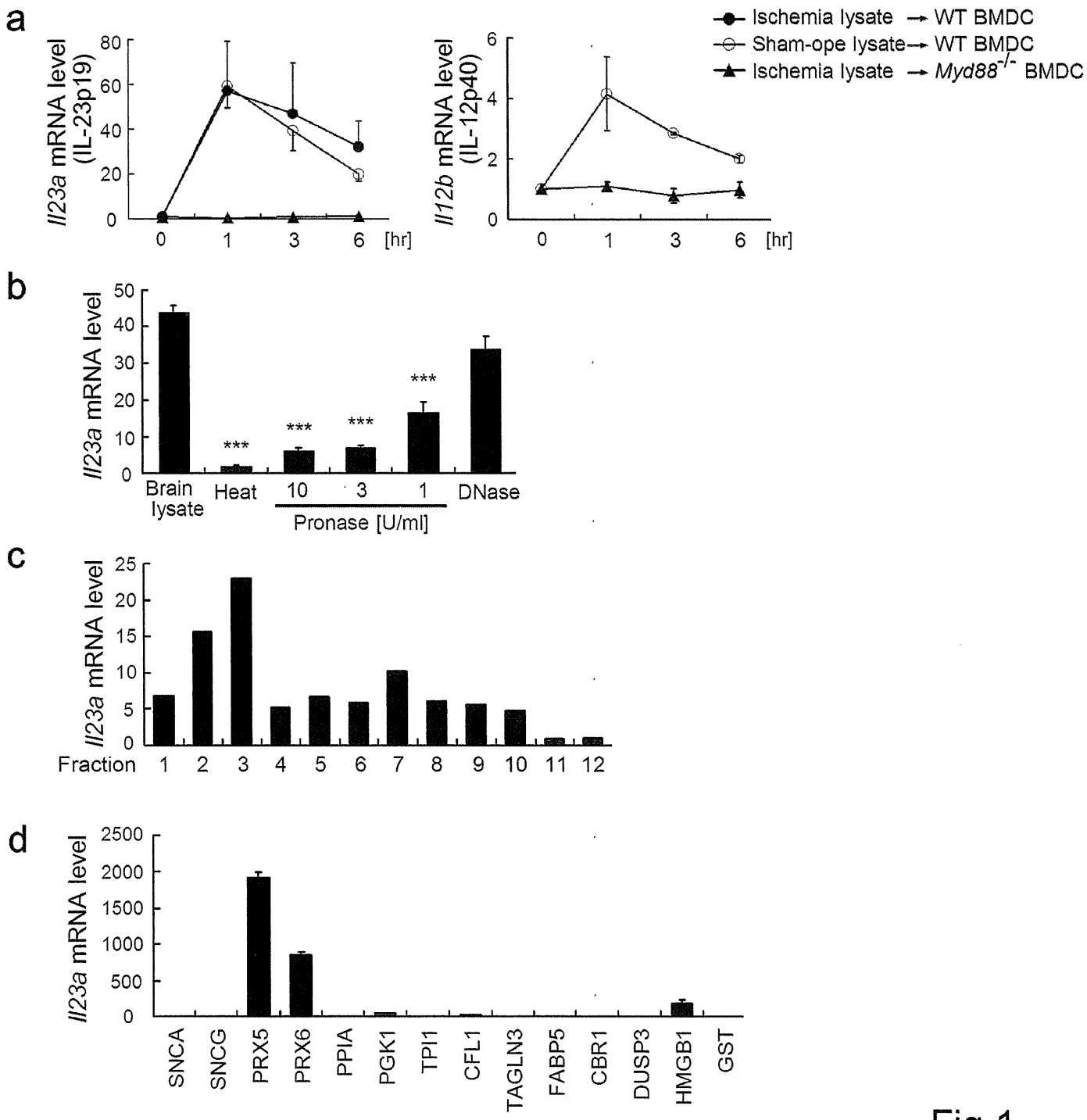
a
Ischemia lysate → WT BMDC
Sham-ope lysate → WT BMDC
Ischemia lysate → Myd88-/- BMDC
Il23a mRNA level (IL-23p19)
Il12b mRNA level (IL-12p40)
[hr]
b
Il23a mRNA level
Brain lysate
Heat
10
3
1
DNase
Pronase [U/ml]
***
c
Il23a mRNA level
Fraction
d
Il23a mRNA level
SNCA
SNCG
PRX5
PRX6
PPIA
PGK1
TPI1
CFL1
TAGLN3
FABP5
CBR1
DUSP3
HMGB1
GST

Fig.1

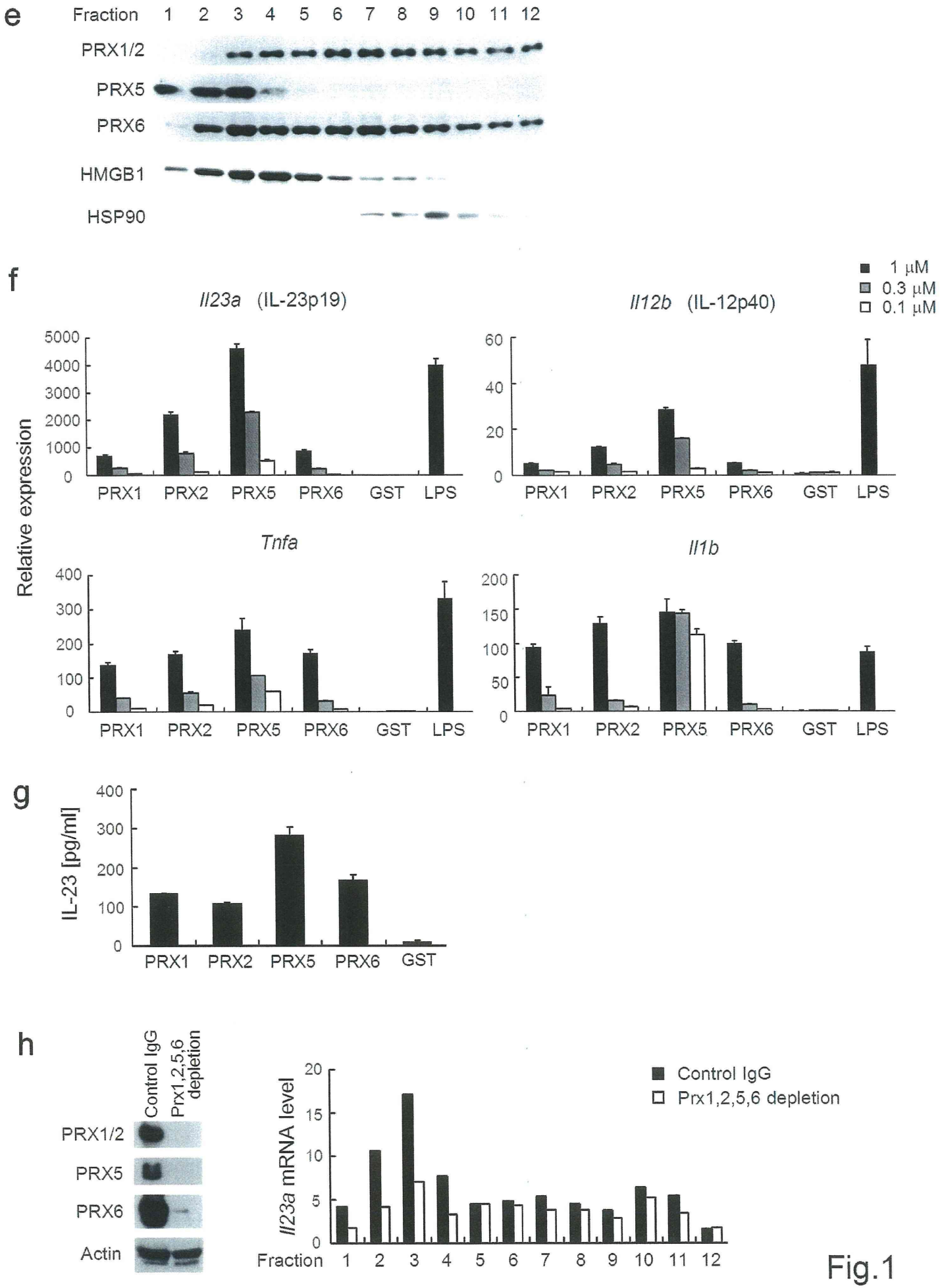
e
Fraction 1 2 3 4 5 6 7 8 9 10 11 12
PRX1/2
PRX5
PRX6
HMGB1
HSP90
f
1 μM
0.3 μM
0.1 μM
Il23a (IL-23p19)
Il12b (IL-12p40)
Tnfa
Il1b
Relative expression
PRX1 PRX2 PRX5 PRX6 GST LPS
g
IL-23 [pg/ml]
PRX1 PRX2 PRX5 PRX6 GST
h
Control IgG
Prx1,2,5,6 depletion
PRX1/2
PRX5
PRX6
Actin
Il23a mRNA level
Control IgG
Prx1,2,5,6 depletion
Fraction 1 2 3 4 5 6 7 8 9 10 11 12

Fig.1

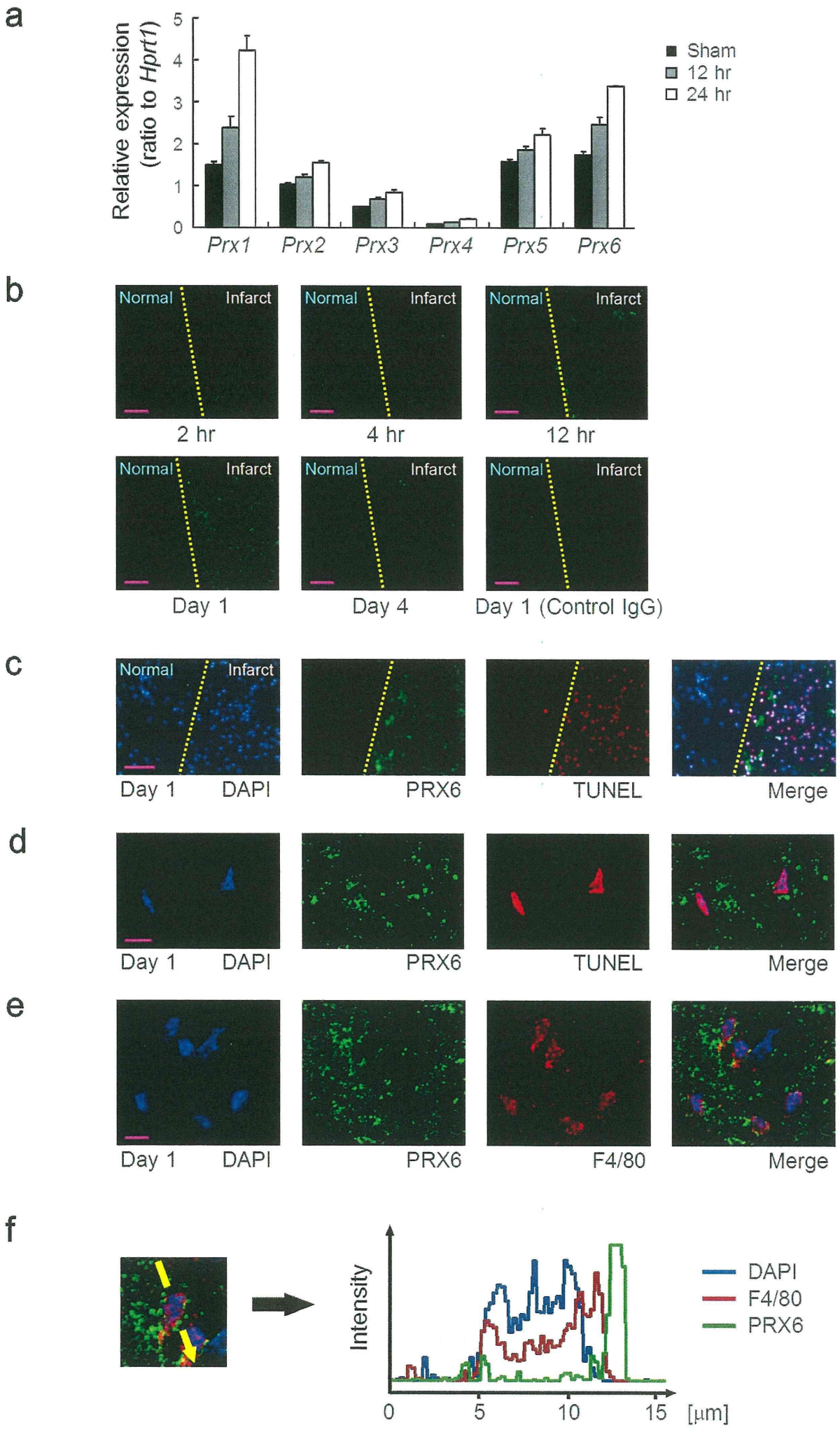
a
Relative expression (ratio to Hprt1)
0
1
2
3
4
5
Prx1
Prx2
Prx3
Prx4
Prx5
Prx6
Sham
12 hr
24 hr
b
Normal
Infarct
2 hr
4 hr
12 hr
Day 1
Day 4
Day 1 (Control IgG)
c
Day 1
DAPI
PRX6
TUNEL
Merge
d
Day 1
DAPI
PRX6
TUNEL
Merge
e
Day 1
DAPI
PRX6
F4/80
Merge
f
Intensity
0
5
10
15
[μm]
DAPI
F4/80
PRX6

Fig.2

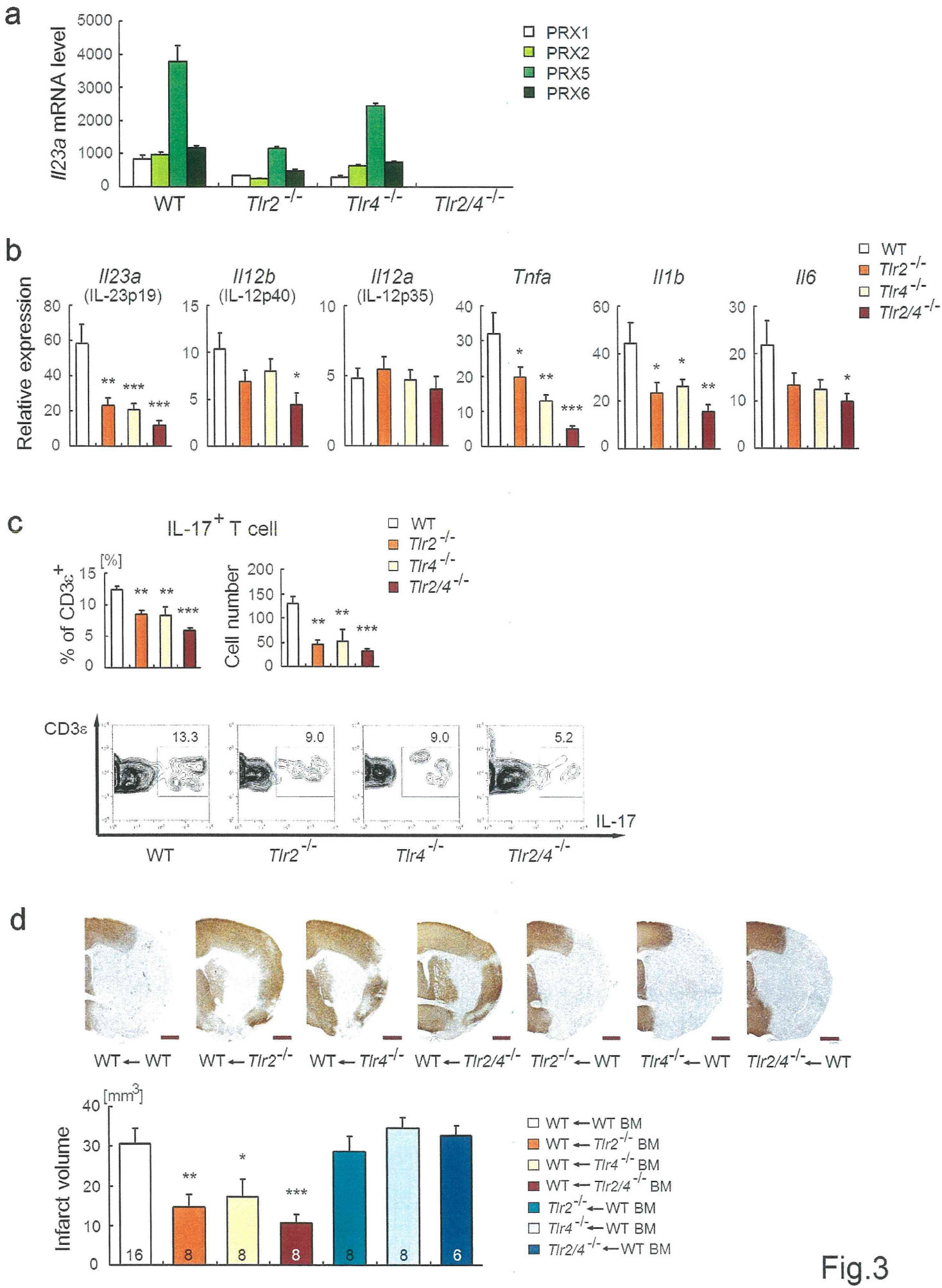
a
Il23a mRNA level
5000
4000
3000
2000
1000
0
PRX1
PRX2
PRX5
PRX6
WT
Tlr2 -/-
Tlr4 -/-
Tlr2/4 -/-
b
Relative expression
Il23a (IL-23p19)
Il12b (IL-12p40)
Il12a (IL-12p35)
Tnfa
Il1b
Il6
WT
Tlr2 -/-
Tlr4 -/-
Tlr2/4 -/-
c
IL-17+ T cell
% of CD3ε+
[%]
Cell number
WT
Tlr2 -/-
Tlr4 -/-
Tlr2/4 -/-
CD3ε
IL-17
13.3
9.0
9.0
5.2
WT
Tlr2 -/-
Tlr4 -/-
Tlr2/4 -/-
d
WT ← WT
WT ← Tlr2 -/-
WT ← Tlr4 -/-
WT ← Tlr2/4 -/-
Tlr2 -/- ← WT
Tlr4 -/- ← WT
Tlr2/4 -/- ← WT
Infarct volume
[mm3]
16
8
8
8
8
8
6
WT ← WT BM
WT ← Tlr2 -/- BM
WT ← Tlr4 -/- BM
WT ← Tlr2/4 -/- BM
Tlr2 -/- ← WT BM
Tlr4 -/- ← WT BM
Tlr2/4 -/- ← WT BM

Fig.3

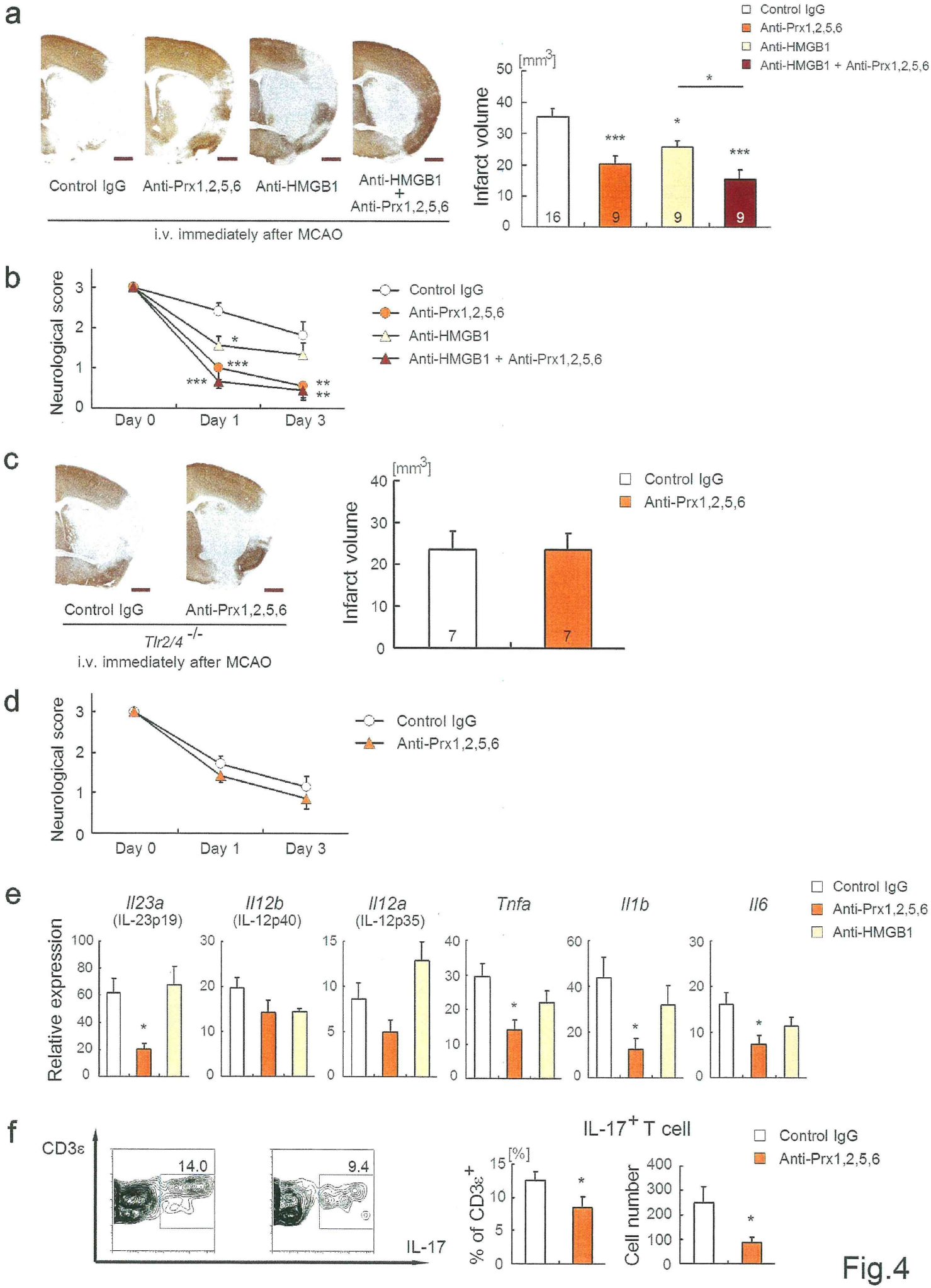
a
Control IgG
Anti-Prx1,2,5,6
Anti-HMGB1
Anti-HMGB1 + Anti-Prx1,2,5,6
Control IgG
Anti-Prx1,2,5,6
Anti-HMGB1
Anti-HMGB1
+
Anti-Prx1,2,5,6
i.v. immediately after MCAO
Infarct volume
[mm3]
50
40
30
20
10
0
16
9
9
9
*
*
***
***
b
Neurological score
3
2
1
0
Day 0
Day 1
Day 3
Control IgG
Anti-Prx1,2,5,6
Anti-HMGB1
Anti-HMGB1 + Anti-Prx1,2,5,6
c
Control IgG
Anti-Prx1,2,5,6
Tlr2/4 -/-
i.v. immediately after MCAO
Infarct volume
[mm3]
40
30
20
10
0
7
7
d
Neurological score
Day 0
Day 1
Day 3
Control IgG
Anti-Prx1,2,5,6
e
Il23a
(IL-23p19)
Il12b
(IL-12p40)
Il12a
(IL-12p35)
Tnfa
Il1b
Il6
Relative expression
Control IgG
Anti-Prx1,2,5,6
Anti-HMGB1
f
CD3ε
14.0
9.4
IL-17
IL-17+ T cell
% of CD3ε+
[%]
Cell number
Control IgG
Anti-Prx1,2,5,6

Fig.4

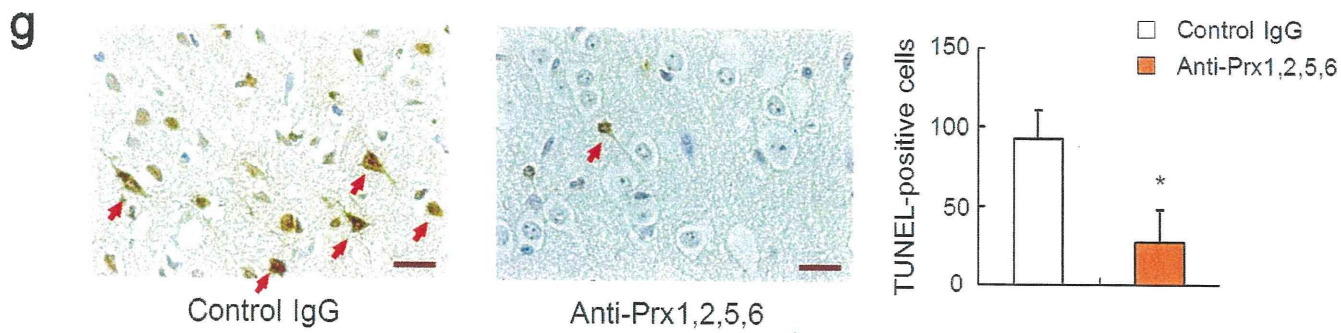
g
Control IgG
Anti-Prx1,2,5,6
TUNEL-positive cells
150
100
50
0
Control IgG
Anti-Prx1,2,5,6
*

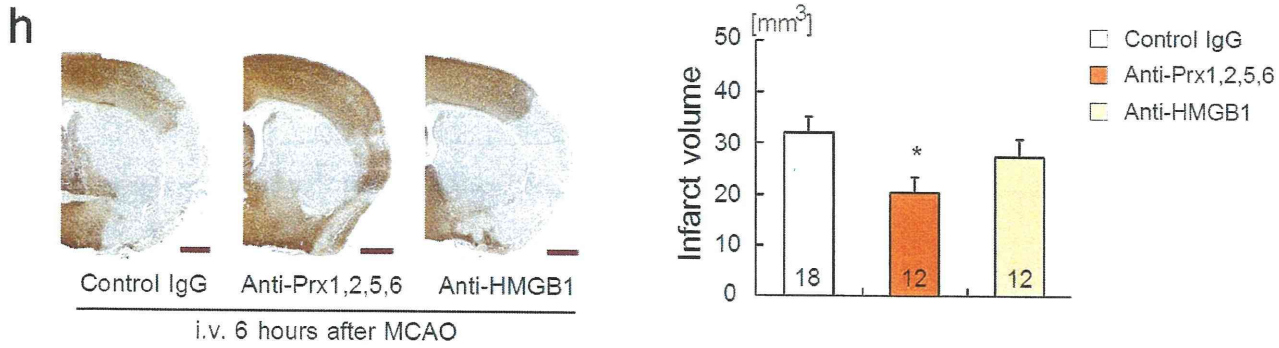
h
Control IgG
Anti-Prx1,2,5,6
Anti-HMGB1
i.v. 6 hours after MCAO
Infarct volume
[mm3]
50
40
30
20
10
0
18
12
12
*
Control IgG
Anti-Prx1,2,5,6
Anti-HMGB1

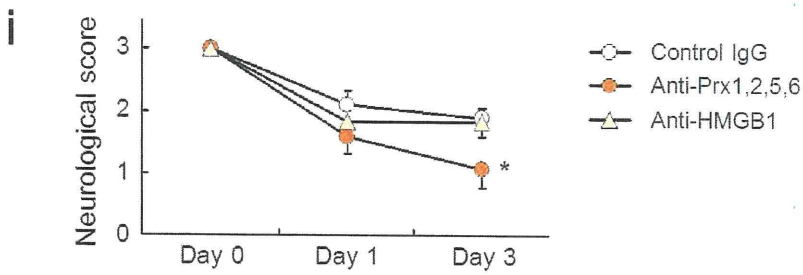
i
Neurological score
3
2
1
0
Day 0
Day 1
Day 3
*
Control IgG
Anti-Prx1,2,5,6
Anti-HMGB1

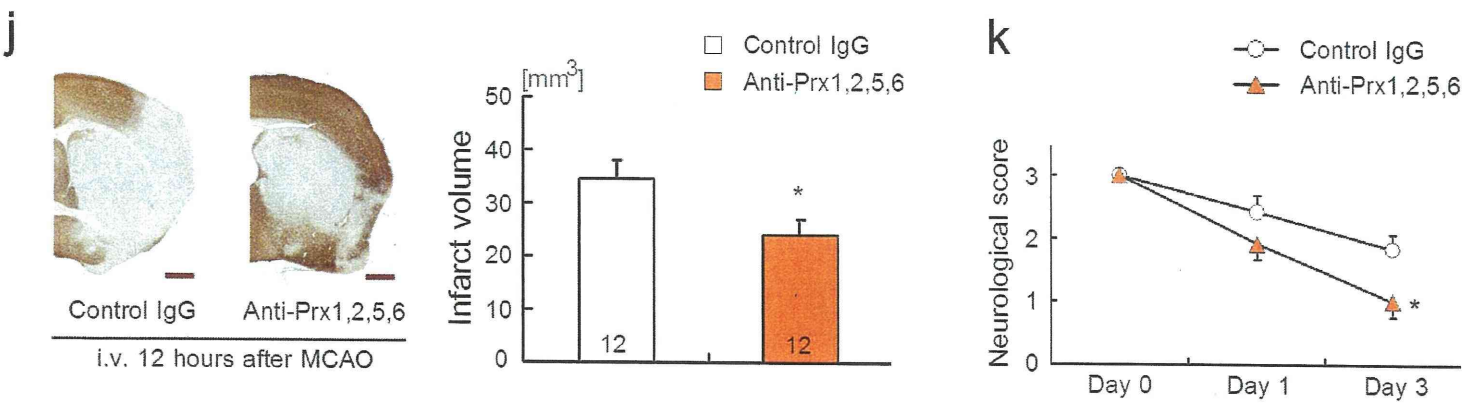
j
Control IgG
Anti-Prx1,2,5,6
i.v. 12 hours after MCAO
Infarct volume
[mm3]
50
40
30
20
10
0
12
12
*
Control IgG
Anti-Prx1,2,5,6
k
Control IgG
Anti-Prx1,2,5,6
Neurological score
3
2
1
0
Day 0
Day 1
Day 3
*

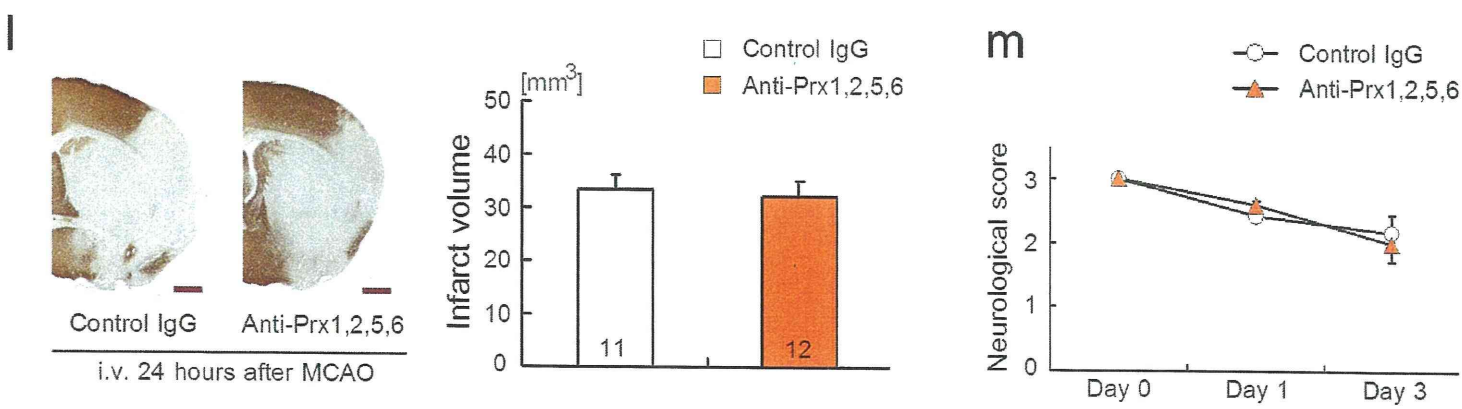
l
Control IgG
Anti-Prx1,2,5,6
i.v. 24 hours after MCAO
Infarct volume
[mm3]
50
40
30
20
10
0
11
12
Control IgG
Anti-Prx1,2,5,6
m
Control IgG
Anti-Prx1,2,5,6
Neurological score
3
2
1
0
Day 0
Day 1
Day 3

Fig.4

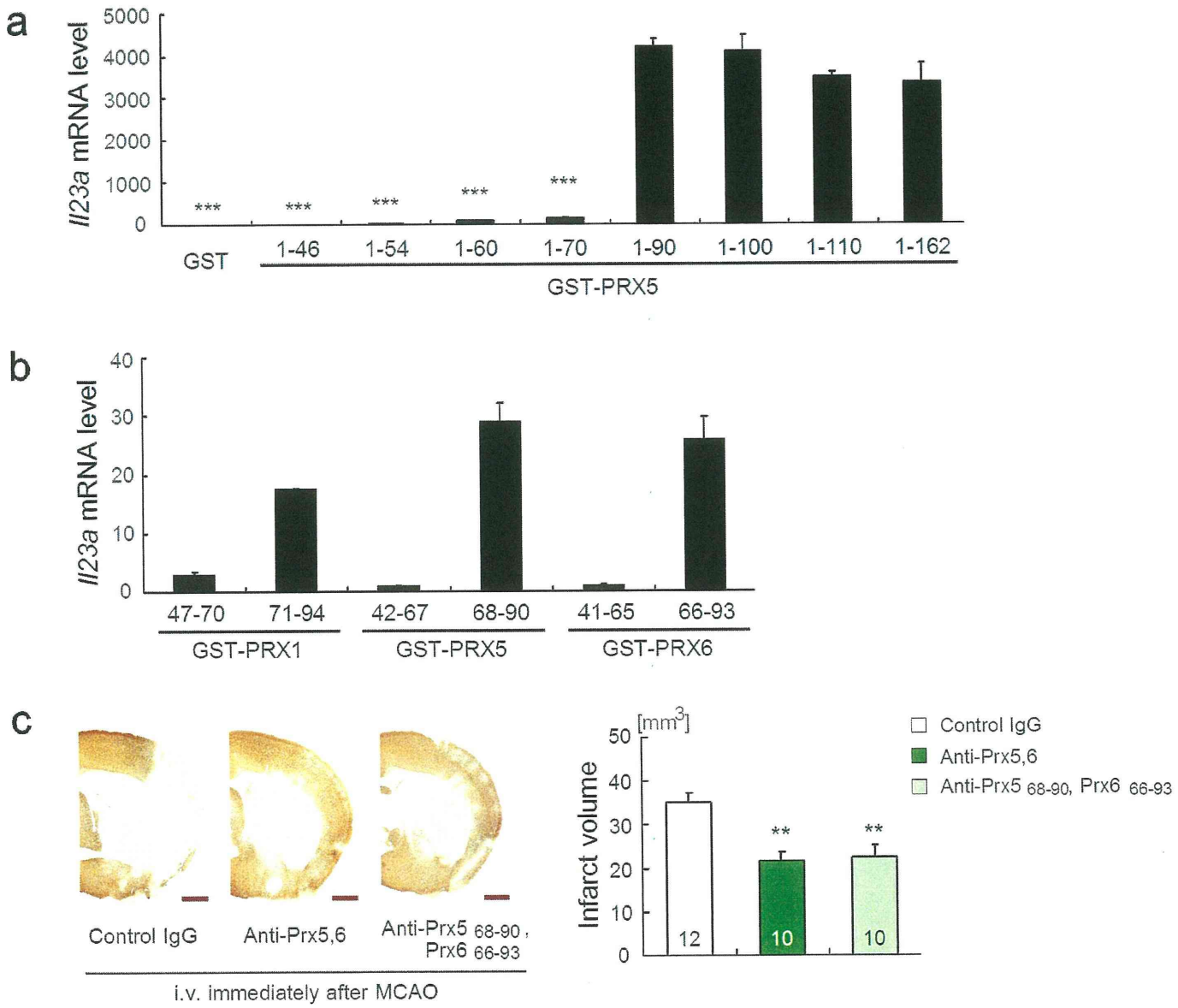
a
Il23a mRNA level
5000
4000
3000
2000
1000
0
***
GST
1-46
1-54
1-60
1-70
1-90
1-100
1-110
1-162
GST-PRX5
b
Il23a mRNA level
40
30
20
10
0
47-70
71-94
42-67
68-90
41-65
66-93
GST-PRX1
GST-PRX5
GST-PRX6
c
Control IgG
Anti-Prx5,6
Anti-Prx5 68-90 , Prx6 66-93
i.v. immediately after MCAO
Infarct volume
[mm3]
50
40
30
20
10
0
12
10
10
**
Control IgG
Anti-Prx5,6
Anti-Prx5 68-90, Prx6 66-93
d
Neurological score
3
2
1
0
Day 0
Day 1
Day 3
*
**
***
Control IgG
Anti-Prx5,6
Anti-Prx5 68-90, Prx6 66-93

Fig.5

Peroxiredoxin family proteins are key initiators of post-ischemic inflammation in the brain

Takashi Shichita, Eiichi Hasegawa, Akihiro Kimura, Rimpei Morita, Ichiro Takada, Takashi Sekiya, Hiroaki Ooboshi, Takanari Kitazono, Toru Yanagawa, Tetsuro Ishii, Hideo Takahashi, Shuji Mori, Masahiro Nishibori, Kazumichi Kuroda, Kensuke Miyake, Shizuo Akira, and Akihiko Yoshimura

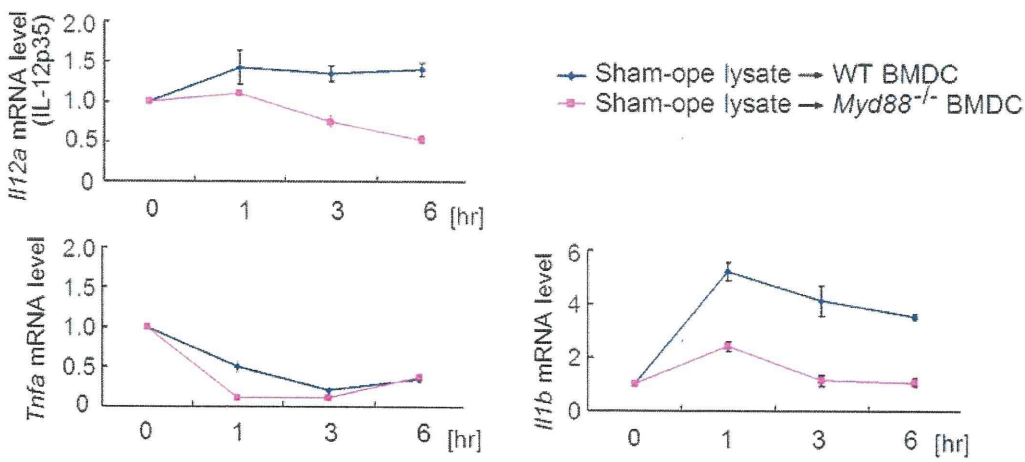

Supplementary Figure 1. The time course of IL-12p35, TNF-α, and IL-1β mRNA expression levels in WT and *Myd88*$^{-/-}$ BMDC induced by the addition of sham-operated brain lysate (n = 3, each).

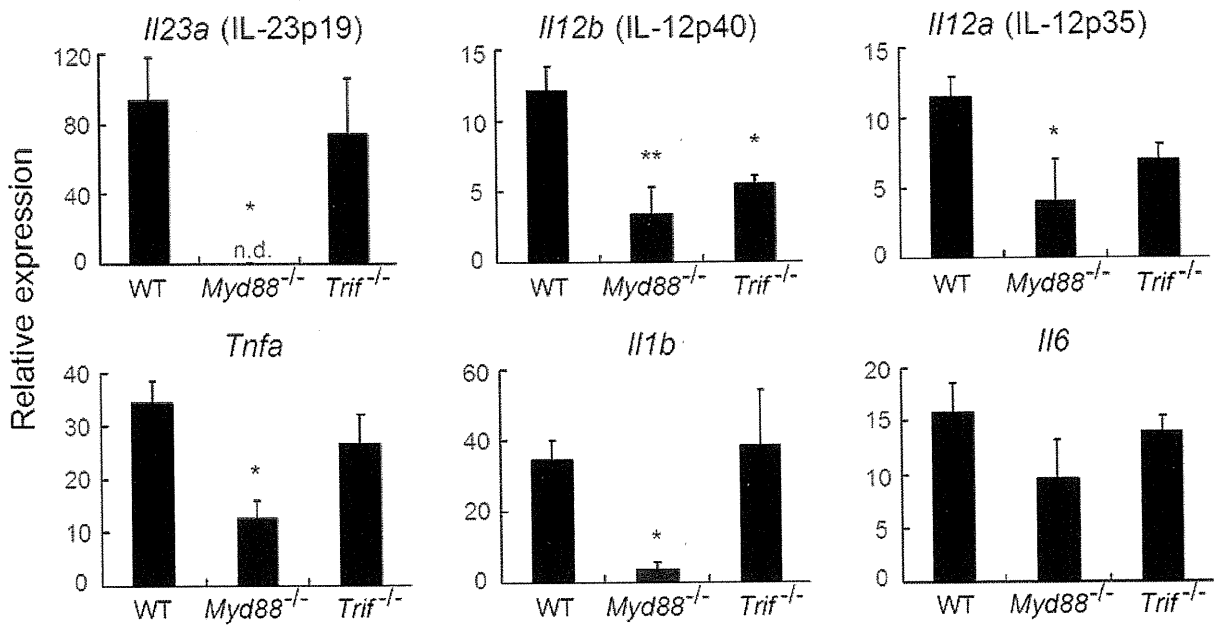

Supplementary Figure 2. The mRNA expression levels of inflammatory cytokines in the infiltrating immune cell in the ischemic brain on day 1. WT, $n = 5$; *Myd88*$^{-/-}$ and *Trif*$^{-/-}$, $n = 3$. *$p <$ 0.05, **$p < 0.01$ vs. wild-type [one-way ANOVA with Dunnett's correction; error bars represent s.e.]. n.d.: not detected.

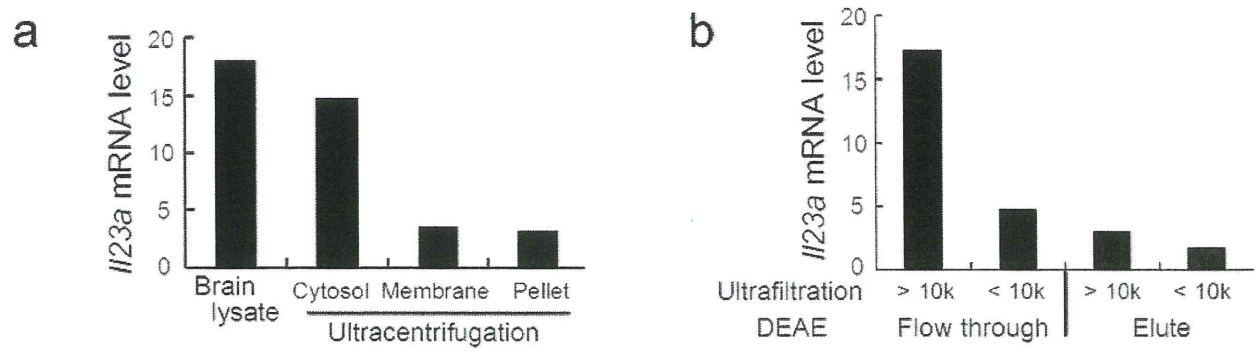

Supplementary Figure 3. (**a**) The IL-23p19 mRNA expression levels in BMDC 1 hour after the stimulation by each fraction of ultracentrifugation. (**b**) The IL-23p19-inducing activity of each fraction by ultrafiltration (10 kDa cut-off) and DEAE Sepharose (representative data of three independent experiments).

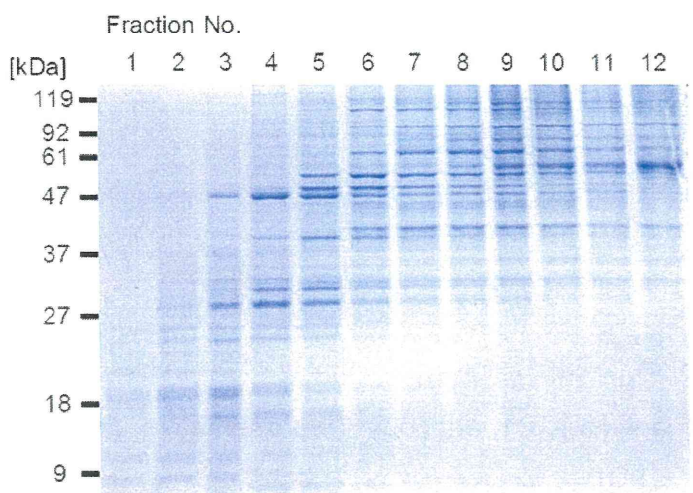

Supplementary Figure 4. SDS-PAGE analysis with CBB staining of each sucrose gradient fraction of the brain lysate (representative data of five independent experiments).

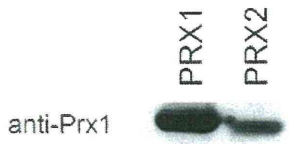

Supplementary Figure 5. Western blot analysis using rabbit polyclonal anti-Prx1 antibody. Due to the high homology between Prx1 and Prx2, anti-Prx1 antibody could also detect Prx2.

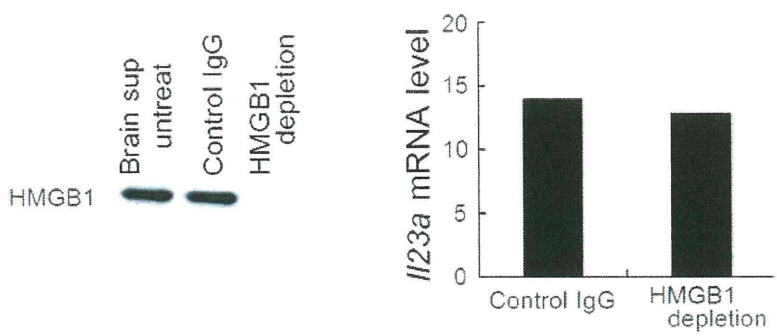

Supplementary Figure 6. The comparison of IL-23p19-inducing activity of brain lysate after the immunoprecipitation with control IgG or anti-HMGB1 antibody (representative data of two independent experiments). The complete depletion of HMGB1 was confirmed by Western blot analysis.